Immune Prognostic Implications of PSMD14 and Its Associated Genes Signatures in Hepatocellular Carcinoma

Tian Chuan (502485085@qq.com)
NANJING UNIVERSITY https://orcid.org/0000-0003-3255-6487
Abudoureyimu Mubalake
Nanjing University
Lin Xinrong
Nanjing University
Zhou Hao
Nanjing Medical University
Chu Xiaoyuan
Nanjing University
Wang Rui
Nanjing University

Primary research

Keywords: HCC, PSMD14, TCGA, ICGC, Prognosis, Immune infiltrates

Posted Date: November 6th, 2020

DOI: https://doi.org/10.21203/rs.3.rs-101311/v1

Abstract

Background

PSMD14 played a vital roles initiation and progression of hepatocellular carcinoma (HCC). However, PSMD14 and its-related genes for the immune prognostic implications of HCC patients have rarely been analyzed. Therefore, we aimed to explore gene signatures and immune prognostic values of PSMD14 and its-related genes in HCC.

Methods

Analyzed the expression of PSMD14 in multiple databases, and clinicopathologic characteristics associated with PSMD14 overall survival using Wilcoxon signed-ranktest, logistic and Cox regression, Kaplan-Meier method. An immune prognostic signature (including RBM45, PSMD1, OLA1, CCT6A, LCAT and IVD) was constructed and validated using the co-expression and cox regression analyses in TCGA, ICGC and TIMER datasets and CIBERSORT computational methods. Gene Set Enrichment Analysis (GSEA) was performed using TCGA data set. RT-PCR further validates the expression of seven immune genes in Hepatocellular carcinoma cells.

Results

Increased PSMD14 expression in HCC was significantly associated with poor prognosis and clinicopathologic characteristics (grade, histologic stage, surgical approach and T stage, all p-values < 0.05). A total of six PSMD14-related genes were detected, which markedly related to overall survival and immune infiltrating levels in HCC patients. Using cox regression analysis, the PSMD14 and its-related genes were found to be an independent prognostic factor for HCC survival. Calibration curves confirmed good consistency between clinical nomogram prediction and actual observation. Immune prognostic model suggests that patients in the high-risk group shown significantly poorer survival than patients in the low-risk group.

Conclusion

We screened potential immune prognostic genes and constructed and verified a novel PSMD14-based prognostic model of HCC, which provides new potential prognostic biomarkers and therapeutic targets and lays a theoretical foundation for immunotherapy of HCC.

Introduction

Hepatocellular carcinoma (HCC) is one of the most common malignancy in the world and the high rate of metastasis is a vital biological feature that leads to unfavorable prognosis (1-2). Although surgery, radiofrequency ablation and chemoembolization have been widely applied for HCC treatment, the survival rate of HCC patients is still low, partly due to high heterogeneity of HCC (3-4). Furthermore, due to the fact that biological processes involved in the occurrence and progression of HCC are very

complicated, no effective prognostic biomarker have yet been found (5). Therefore, it is necessary to explore the new HCC-related molecules for the diagnosis, prognosis and treatment of HCC.

The deubiquitinase (DUB) 26S proteasome non-ATPase regulatory subunit 14 (PSMD14, RPN11 or POH1), belongs to the JAMM domain metalloprotease family of DUBs and is an important part of 19S regulatory cap in 26S proteasome (6). PSMD14 has been confirmed to play vital roles in gene ontology and related pathway, including protein stability (7), tumour formation (8), transcriptional regulation (9), double-strand DNA break repair (10), senescence (11), apoptosis and resistance (12), growth and metastasis (6), BMP6 signaling (7), TGF-β signaling (9). Recently, it has been found that PSMD14 is overexpressed in many human cancers, such as HCC, colorectal cancer, multiple myeloma, esophageal squamous cell carcinoma and breast cancer, which are related to the poor prognosis of the patients (6,7,12-14). PSMD14 acts as an oncogene promotes tumor progression by deubiquitinating different protein substrates. For example, Deubiquitinase PSMD14 positively regulates the initiation of the BMP6 signalling pathway, resulting in increased stability of the ALK2. Either PSMD14 or ALK2 depletion significantly decreases colorectal cancer growth and chemoresistance (7). GRB2 is an oncoprotein that enhances hepatocellular carcinoma growth and metastasis. PSMD14 stabilizes and inhibits the degradation of GRB2 through deubiquitination, which is an oncoprotein enhances hepatocellular carcinoma growth and metastasis (6). POH1 deubiquitinates the TGF-β receptors and CAV1, contributes to hyperactivation of TGF-β signaling and facilitates hepatocellular carcinoma metastasis, which it negatively regulates lysosome pathway-mediated turnover of TGF-β receptors (9). Other mechanisms of the contribution of PSMD14 in the progression of HCC remains to be further explored.

Here, we evaluated PSMD14 mRNA and protein levels and prognostic value in multiple databases and found that increased PSMD14 expression is associated with poor survival of HCC. Moreover, we screened prognostic genes signature closely related to PSMD14 through bioinformatics analysis then constructed the PSMD14-related prognostic model. We validated our model both in The Cancer Genome Atlas (TCGA) and independent International Cancer Genome Consortium (ICGC) database. At last, we confirmed the correlation between PSMD14 expression with clinicopathological characteristics, signatures (RBM45, PSMD1, OLA1, CCT6A , LCAT and IVD) and immune infiltration of hepatocellular carcinoma patients. In conclusion, our study confirms the important role of PSMD14 and its associated genes in Liver cancer as well as correlated with prognosis and immune infiltrating levels in HCC patients, providing new insights relevant to individualized treatment.

Materials And Methods

Cell culture

Human HCC cell lines, HepG2 and Hep3B, were obtained from the Shanghai Cell Bank of Chinese Academy of Sciences (Shanghai, China). The liver cell line, L02, was purchased from Chen Xi Research Group Nanjing University School of the college of Life Sciences. Each cell line was cultured in Dulbecco's modified Eagle medium (DMEM, Invitrogen, USA) supplemented with 10% fetal bovine serum (FBS,

Hyclone) as well as 100 u/ml penicillin and 100 ug/ml streptomycin. All of the cells were maintained in a humidified incubator at 37°C with 5% CO_2.

RNA extraction and Quantitative Real-Time PCR

Total RNA was isolated from the tissue samples and cultured cells using TRIzol reagent (Invitrogen, Carlsbad, CA, USA) according to the manufacturer's insstructions. The

concentration of extracted RNA was measured using a NanoDrop ND-1000 Spectrophotometer (Agilent, Santa Clara, CA, USA). RNA was reverse transcribed into complementary DNA (cDNA) using the PrimeScript RT reagent kit with gDNA Eraser

(Takara, Dalian, China) by incubating the mixture at 37˚C for 15 min, 85˚C for 5 sec at 4˚C. When the temperature reaches 4˚C this process ends.

Quantitative PCR (qPCR) was performed using the SYBR PrimeScript RT-PCR kit (Takara, Shiga, Japan) and the ABI 7500 System (Applied Biosystems, Foster City, CA, USA) according to manufacturer's instructions. The relative expression was calculated via the comparative cycle threshold (CT) method and was normalized to the expression of GAPDH. The primers used are listed in Table 5. Reaction conditions were as follows: 95˚C for 30 sec, followed by 40 cycles of 95˚C for 5 sec and 60˚C for 34 sec. The differential expression level was calculated using the $2^{-\Delta\Delta Ct}$ formula. All the experiments were conducted at least 3 times.

Oncomine database

PSMD14 expression levels were identified in the Oncomine database (https://www.oncomine.org/resource/login.html) in various common of cancers. The data is defined as a P-value of 0.01, a fold change of 1.5, a top 10% gene ranking, and the data has to be from mRNA.

PSMD14 mRNA expression and survival in public databases

To investigate the expression level and prognostic role of PSMD14 mRNA in HCC, the Human Protein Atlas database (http://www.proteinatlas.org), LinkedOmics (http://www.linkedomics.org/admin.php), the Cancer Genome Atlas (TCGA) database (http://cancergenome.nih.gov/), the International Cancer Genome Consortium (ICGC) database (https://dcc.icgc.org/) were used.

TIMER database

We analyzed the correlation between signature genes expression and 6 types of immune infiltrating cells (B cells, CD4+ T cells, CD8+ T cells, neutrophils, macrophages and dendritic cells) in HCC patients via The Tumor Immune Estimation Resource (TIMER) algorithm database (https://cistrome. shinyapps.io/timer/). Tumor purity is a vital factor that influences the analysis of tumor immune infiltration by genomic approaches.

Tumor-infiltrating immune cell

CIBERSORT computational method was applied for estimating the TIC (tumor-infiltrating immune cell) abundance profile in all tumor samples, which followed by quality filtering that only 374 tumor samples with $p < 0.05$ were selected for the following analysis.

Data collection

RNA-sequencing and clinical information for hepatic carcinoma were acquired from the Cancer Genome Atlas (TCGA) database and The International Cancer Genome Consortium (ICGC) database. The clinical features of patients with hepatic carcinoma in the TCGA cohorts are presented in **Table 1**.

Selection of immune-related prognostic genes

Genes significantly associated with PSMD14 (Pearson | R | > 0.4, p < 0.001) were filtered by Pearson correlation analysis in TCGA data sets. The top 10 genes that were positively and negatively correlated with PSMD14 were selected for further analysis.

Identification and validation of the prognostic gene signature

Using univariate and least absolute shrinkage and selection operator (LASSO) COX regression, we filter the independent risk prognostic genes. Moreover, multivariate COX regression was used to identify corresponding coefficients of HCC prognostic signature using the R package “glment”, “survminer” and “survival”. The risk score of every patient was calculated from the TCGA and ICGC database based on the signature. With the median score as cut-off value, all samples were randomly separated to high- and low-risk sets. In addition, survival analysis was evaluated for each set using the Kaplan-Meier curve and log-rank test. The receiver operating characteristic (ROC) curve and the area under the curve (AUC) were drawn using the R package “survivalROC”.

Development of nomogram

We constructed a nomogram for age, gender, stage, T, N, M, and risk score using the survival and the rms package of R. Next, we used a calibration curve to assess the concordance between actual and predicted survival. In addition, The concordance index (C-index) was computed to evaluate the model performance for predicting prognosis, which was ranged from 0.5 to 1.0. Value of 0.5 and 1.0 represents a random chance and an excellent capacity for predicting survival with the model, respectively.

Gene set enrichment analyses

Gene set enrichment analysis (GSEA) was conducted to identify gene sets that differed significantly between the high- and low-risk patient groups, using GSEA 4.0.3 software (http://www.broadinstitute.org/gsea/index.jsp). In the analysis results, it was generally believed that the pathways were significantly enriched when |NES| > 1, NOM p-value < 0.05, and FDR q-value < 0.25.

Statistical analysis

All statistics were executed using the R software (v.3.4.3). Clinicopathologic characteristics associated with PSMD14 overall survival were analyzed using the Wilcoxon signed-ranktest, logistic and Cox regression, Kaplan-Meier method. In addition, x2 test was used to check the association of risk scores with clinical characteristics and univariate and multivariate Cox proportional hazard regression analysis was performed to evaluate the association between risk score and OS. The Receiver Operating Characteristic (ROC) analysis was used to examine the sensitivity and specificity of survival prediction using the gene signature risk score. An area under the ROC curve (AUC) served as an indicator of prognostic accuracy. P-values < 0.05 were considered statistically significant.

Results

Patients characteristics

As shown in Table 1, 418 primary tumors with both gene expression and clinical data were downloaded from TCGA (LIHC-CHOL) data in November 2019. The median age was 61 years old at diagnosis. Moreover, Histopathologic distribution of HCC included well-differentiated (14.8%), moderately differentiated (81.7%) and poorly differentiated (3.5%). The cancer status included 254 tumor-free (65.6%) and 133 with tumor (34.4%). Stage I disease was found in 194 patients (49.2%), stage II in 98 (24.9%), stage III in 90 (22.8%) and stage IV in 12 (3.1%). Grade I disease was found in 55 patients (14.8%), Grade II in 180 (48.4%), Grade III in 124 (33.3%) and Grade IV in 13 (3.5%).The Vascular invasion include 17 Macro (5.3%), 94 Micro (29.3%) and 210 NO (65.4%). Most tumors (87.8%, n=367) were of Hepatocellular Carcinoma (HCC), 9.8% (n=41) were Cholangiocarcinoma (CHOL), 1.7% (n=7) were Hepatocholangiocarcinoma (Mixed) and 0.7% (n=3) were Fibrolamellar Carcinoma (FLC). Tumor size (≤5cm, 74.9%, n=311) and (>5cm, 25.1%, n=104). Eight of 298 (2.7%) cases had lymph node metastases. Eight of 311 (2.6%) cases had distant metastases.

PSMD14 mRNA expression

Oncomine database analysis exhibits significantly up-regulation of PSMD14 in 2 Liver cancer data set compared to the normal liver tissues (Figure 1A). Complementary, PSMD14 mRNA expression was higher in most tumors, such as bladder cancer, brain and CNS, breast cancer, cervical, colorectal cancer, head and neck cancer, kidney cancer, liver cancer, lung cancer, lymphoma, myeloma, pancreatic cancer and sarcoma. To further assess PSMD14 expression of liver cancer, we verified PSMD14 mRNA expression by TIMER data set (Figure 1B). PSMD14 mRNA expression was significantly higher in Liver Hepatocellular Carcinoma (LIHC) compared with adjacent normal tissues.

PSMD14 expression and its clinical significance in HCC

To further assess the role of PSMD14 in HCC, we first analyzed four independent microarray datasets from Oncomine database. The median rank of PSMD14 in up-regulated genes of HCC was 1197.5 based

on a meta analysis across the four datasets, including 4 analyses using the Oncomine algorithms (760 samples, *P* = 2.96E-5, Figure 2A) (15-17). In the meantime, we examined the protein expression of PSMD14 using the Human Protein Atlas (HPA). Images revealed a markedly high expression of PSMD14 could be observed compared to the normal Liver tissues using the HPA002114 antibody in Liver cancer (Figure 2B). Next, we evaluated PSMD14 mRNA expression compared with normal tissues in multiple HCC studies from TCGA and ICGC databases, and found that the mRNA level of PMSD14 was significantly higher in HCC patients than normal liver tissues (Figure 2C-D). These findings suggested that PSMD14 is highly expressed in HCC and elevated PSMD14 may predict a poor outcome for HCC patients.

We analyzed 377 HCC samples with PSMD14 expression and clinical characteristics from the TCGA database. As shown in Figure 3 (A-D)**.** Significant increase in PSMD14 expression correlated with tumor histological grade (p = 0.046), histological stage (p < 0.001), surgical approach (p = 0.001) and T stage (p = 0.013). Categorical dependent variable using logistic regression, univariate analysis showed that PSMD14 expression was significantly associated with poor prognostic clinicopathologic characteristics (Table 2). Increased PSMD14 expression was significantly associated with grade (OR =1.9 for well vs. moderate), stage (OR = 2.5 for I vs. II, III), surgical approach (OR = 0.26 for HL vs. SSLR), tumor size (OR = 1.65 for ≤5cm vs. > 5cm) in HCC (all p-values < 0.05). The results suggested that HCC with high PSMD14 expression was progressed to a more advanced stage than those with low PSMD14 expression.

Survival and independent prognostic analysis

Kaplan-Meier survival analysis indicated that HCC with PSMD14-high had a poor prognosis than the PSMD14-low in TCGA and ICGC database in Figure 3 (E-F) (p < 0.001). The univariate analysis revealed that PSMD14-high correlated significantly with a poor OS (hazard ratio (HR): 2.17; 95% confidence interval (CI): 1.32-3.57; p = 0.002). Other clinicopathologic variables related to poor survival include status, stage, T stage and distant metastasis. Multivariate analysis with HR of 1.9 shown that the PSMD14 remained independently associated with overall survival (CI: 1.08-3.33, p = 0.026), along with status in TCGA (Table 3). Therefore, we first revealed that PSMD14 was associated with poor prognosis, as an independent prognostic factor for HCC survival.

Construction and validation of signature

We selected the genes signatures associated with PSMD14 in the TCGA-LIHC database. A total of 2478 PSMD14-associated genes (Pearson |R| > 0.4, p < 0.001) were chosen to generate prognosis gene signatures and the top 10 positively and negatively genes were selected for further analysis (Figure 4A). All genes were analyzed by univariate Cox regression. A total of 17 genes were significantly related to the OS in TCGA-LIHC database (Figure 4B). Then, the LASSO COX regression analysis and the regression coefficient was computed, the model achieved the best performance at 6 genes (Figure 4C). Finally, we constructed a risk signature for HCC using multivariate COX regression (Table 4). All patients were divided into high- and low-risk sets based on median risk score in the TCGA and ICGC database. Status, survival time and gene expression levels of patients were shown in TCGA (Figure 4D) and ICGC (Figure 4E).

The survival analysis indicated that the OS of the low-risk set was better than that of high-risk set in the TCGA database ($P < 0.001$) (Figure 5A). The results were consistent in the ICGC database (P < 0.001) (Figure 5B). The area under the ROC curve (AUC) for 1-, 3-, and 5-year OS were 0.723, 0.653, 0.645, 0.657, 0.705, 0.683 in the TCGA (Figure 5C) and ICGC (Figure 5D) cohorts, respectively. Together, Results revealed that the signature showed excellent performance for OS prediction.

Univariate and multivariate COX regression analysis

Univariate Cox regression indicated that stage, T stage, M stage and risk score in the TCGA database (stage: P < 0.001; T stage: P < 0.001; M stage: P = 0.026; risk score: P < 0.001; Figure 6A), and gender, stage, risk score in the ICGC database (gender: P =0.039; stage: P < 0.001; risk score: P < 0.001; Figure 6C) were predictors for OS. Moreover, multivariate Cox regression analysis verified that age (HR = 1.019, 95% CI (1.003- 1.034); P = 0.017) and risk score (HR = 1.545; 95% CI (1.354-1.763); P < 0.001; Figure 6B) were significant independent risk factors in the TCGA database. Multivariate Cox regression further showed that gender (HR = 0.372, 95% CI (0.196-0.707); P =0.003); stage (HR = 2.320, 95% CI (1.599-3.367); P < 0.001); priorMalignancy (HR = 2.500, 95% CI (1.065-5.868); P =0.035) and risk score (HR = 1.094; 95% CI (1.031-1.162); P =0.003; Figure 6D) was significant independent risk factors in the ICGC database. These data demonstrated that this signature was an independent risk factor of HCC.

Nomogram construction

Based on the prognostic signature and clinical factors, such as age, gender, vascular invasion, tumor status and stage, a nomogram was constructed (Figure 7A). The calibration curve was used to describe the prediction value of the nomogram and the 45-degree line indicates the actual survival outcomes. The results showed that the nomogram-predicted survival closely matched with the best prediction performance for predicting 1-, 3- and 5-year OS (Figure 7B). The 1-year AUC was 0.765 for nomogram, and 0.481 for age, 0.490 for grade, 0.425 for status, 0.711 for stage. The 3-year AUC was 0.697 for nomogram, and 0.508 for age, 0.525 for grade, 0.567 for status, 0.706 for stage. Moreover, the 5-year AUC was 0.715 for nomogram, and 0.594 for age, 0.508 for grade, 0.607 for status, 0.667 for stage (Figure 7C-E). These showed that compared with a single clinical factor, the nomogram had great predictive accuracy combined the signature and clinical factors.

Model gene verification

Consistent with our results, IVD and LCAT were found to be significantly downexpressed, while CCT6A and OLA1 were significantly overexpressed for liver cancer in the Oncomine (Figure 8A), TIMER (Figure 8B), TCGA (Figure 8C) and ICGC (Figure 8D) database. Though lack in the Oncomine database, the mRNA expression of PSMD1 and RBM45 were also found to be significantly overexpressed for liver cancer in the TIMER, TCGA and ICGC database. Taking together, we further verified aberrant expression of six prognostic genes and found that IVD and LCAT genes were significantly decreased, while CCT6A,OLA1,PSMD1 and RBM45 genes were increased in HCC tissues.

Gene set enrichment analyses

We carried on the Gene Set Enrichment Analysis (GSEA) between PSMD14 (high/low) expression and high/low risk model data sets in TCGA-LIHC. GSEA revealed significant difference (FDR < 0.05, NOM p-val < 0.05) in enrichment of MSigDB Collection (c2.cp.kegg.v7.0.symbols.gmts). We selected the most significantly enriched signaling pathways based on their normalized enrichment score (NES). A great majority of the enriched pathways were metabolism related, such as the purine metabolism, pyrimidine metabolism and ubiquitin mediated proteolysis are differentially enriched in PSMD14 high expression and high-risk group phenotype (Figure 9A). Besides, the glycine serine and threonine metabolism, primary bile acid biosynthesis and retinol metabolism were enriched in PSMD14 low expression and low-risk group phenotype (Figure 9B).

Seven genes expression is correlated with immune infiltration level

We investigated the expression of seven genes (PSMD14, RBM45, PSMD1, OLA1, CCT6A, LCAT and IVD) in human HCC cell lines Hep3B and HepG2. Compared to the normal liver cell L02, IVD and LCAT were significantly downregulated, the PSMD14,PSMD1,RBM45, OLA1 and CCT6A gens were significantly upregulated in the Hep3B and HepG2 cells (Figure 10A).

In addition, we analyzed the correlation between seven prognostic genes (PSMD14, RBM45, PSMD1, OLA1, CCT6A , LCAT and IVD) expression and 6 types of infiltrating immune cells (B cells, CD4 T cells, CD8+ T cells, neutrophils, macrophages and dendritic cells) in LIHC. The results showed that PSMD14 expression levels had a significantly positive correlation with infiltrating levels of B Cell (r = 0.245, P = 4.27e-06), CD8+ T cell (r = 0.205, P = 1.30e-04), CD4+ T cell (r = 0.266, P = 5.57e-07), Macrophage (r = 0.374, P = 9.16e-13), Neutrophils (r = 0.445, P = 3.30e-18) and Dendritic cells (r = 0.317, P = 2.33e-09). RBM45 expression levels had a significantly positive correlation with infiltrating levels of B Cell (r = 0.35, P = 2.39e-11), CD8+ T cell (r = 0.26, P = 1.07e-06), CD4+ T cell (r = 0.367, P = 2.12e-12), Macrophage (r = 0.461, P = 2.55e-19), Neutrophils (r = 0.471, P = 1.72e-20) and Dendritic cells (r = 0.419, P = 6.90e-16). PSMD1 expression levels had a significantly positive correlation with infiltrating levels of B Cell (r = 0.257, P = 1.31e-06), CD8+ T cell (r = 0.192, P = 3.50e-04), CD4+ T cell (r = 0.299, P = 1.55e-08), Macrophage (r = 0.393, P = 4.53e-14), Neutrophils (r = 0.447, P = 2.22e-18) and Dendritic cells (r = 0.355, P = 1.50e-11). OLA1 expression levels had a significantly positive correlation with infiltrating levels of B Cell (r = 0.359, P = 6.46e-12), CD8+ T cell (r = 0.27, P = 3.89e-07), CD4+ T cell (r = 0.328, P = 4.51e-10), Macrophage (r = 0.444, P = 6.18e-18), Neutrophils (r = 0.382, P = 1.98e-13) and Dendritic cells (r = 0.399, P = 1.93e-14). CCT6A expression levels had a significantly positive correlation with infiltrating levels of B Cell (r = 0.322, P = 9.24e-10), CD8+ T cell (r = 0.16, P = 3.06e-03), CD4+ T cell (r = 0.352, P = 1.72e-11), Macrophage (r = 0.462, P = 1.90e-19), Neutrophils (r = 0.367, P = 2.04e-12) and Dendritic cells (r = 0.313, P = 3.45e-09). None of the above five genes had no significant correlations with tumor purity (P >0.05) (Figure 10B-G).

LCAT expression was significantly negatively related to tumor purity (r = -0.124, P = 2.12e-02) and had a significantly negative correlation with infiltrating levels of B Cell (r = -0.197, P = 2.35e-04), CD8+ T cell (r = -0.103, P = 5.59e-02), CD4+ T cell (r = -0.174, P = 1.16e-03), Macrophage (r = -0.244, P = 5.21e-06),

Neutrophils (r = -0.202, P = 1.53e-04) and Dendritic cells (r = -0.194, P = 3.12e-04) (Figure 10F). IVD expression was significantly positive related to tumor purity (r = 0.121, P = 2.45e-02) and had a significantly negative correlation with infiltrating levels of B Cell (r = -0.173, P = 1.31e-03), CD8+ T cell (r = -0.097, P = 7.37e-02), CD4+ T cell (r = -0.135, P = 1.20e-02), Macrophage (r = -0.171, P = 1.49e-03) and Dendritic cells (r = -0.145, P = 7.53e-03) and no significant correlations with Neutrophils (r = -0.065, P = 2.271e-01) (Figure 10H).

Correlation of PSMD14 with the proportion ofTICs

To further confirm the correlation of PSMD14 expression with the proportion of tumor-infiltrating immune subsets was analyzed using CIBERSORT algorithm, and 21 kinds of immune cell profiles in LIHC samples were constructed. The results from the difference and correlation analyses showed that a total of six kinds of TICs were correlated with the expression of PSMD14 (Figure 11). Among them, three kinds of TICs were positively correlated with PSMD14 expression, including Macrophage M0, T cells CD4 memory activated and NK cells resting; three kinds of TICs were negatively correlated with PSMD14 expression, including B cells naïve, NK cells activated and T cells CD4 memory resting. These results further supported that the levels of PSMD14 affected the immune activity of TICs.

Discussion

HCC remains a common malignant tumor in the world, with a low survival rate. Thus, in view of the low survival rate for HCC, investigation of novel biomarkers and models is necessary. Recently, PSMD14-based signatures have revealed excellent potential in prognosis prediction of multiple cancers. The prognosis value of PSMD14 in cancers have been reported, including HCC, esophageal cancer, breast cancer (6,13-14). Our results are in accordance with these studies, implying that PSMD14 could be a potential prognostic gene for HCC (6). To our knowledge, the expression of PSMD14 and its potential immune prognostic impact on HCC has not yet been explored. The present study focused on the potential immune prognostic role of PSMD14 and its associated genes in HCC.

In the present study, we verified the high expression of PSMD14 in liver cancer through Multiple databases, including ONCOMINE, TIMER, HPA, TCGA, ICGC. Bioinformatic analysis from TCGA and ICGC database demonstrated that high expression of PSMD14 in HCC was associated with clinical pathologic characteristics (high grade, histologic stage, surgical approach, T stage), survival time and poor prognosis. Univariate and multivariate COX regression shows PSMD14 as an independent prognostic factor (Table 3). In addition, we identified the PSMD14 associated novel biomarkers base on TCGA data set, and confirmed PSMD14 associated genes model significantly correlated with prognosis using COX regression and LASSO analysis. Finally, six genes (RBM45, PSMD1, OLA1, CCT6A , LCAT and IVD) were selected to fabricate a prognostic signature for HCC, validated its efficiency in TCGA and ICGC data set. A robust nomogram consisted of the 6-genes signature, age, gender, vascular invasion, tumor status and the stage was constructed for prognostic prediction of HCC patients. At the same time, the AUC value of the signature-based nomogram was nearly better than the AUC values of age, grade status and stage in

1-, 3, 5- years. Next, we further verified the mRNA expression of 6-genes (RBM45, PSMD1, OLA1, CCT6A , LCAT and IVD) for HCC patients in the Oncomine, TIMER, TCGA and ICGC database, which is consistent with the results of previous studies (18-21). What's interesting, there are no reports of RBM45 and IVD genes in liver cancer. They may become new targets for the treatment of liver cancer, which need to be further studied.

A total of 7 key prognostic genes of HCC patients were selected in this paper. However, no review had been studied about intriguing mechanisms of these key genes in HCC except PSMD14 and CCT6A. POH1 was first found as a human pad1 homologue in 1997, a previously unidentified component of the human 26S proteasome, that degrades proteins targeted for destruction by the ubiquitin pathway (21). Lv (6) reveal that PSMD14, as a novel posttranslational regulator of GRB2, inhibits degradation of GRB2 via deubiquitinating this oncoprotein in HCC cells. Overexpressed CCT6A contributes to cancer cell growth by affecting the G1-to-S phase transition and predicts a negative prognosis in Hepatocellular Carcinoma. CCT6A may contribute to HCC cell proliferation by accelerating the G1-to-S transition and predicts a negative prognosis in Hepatocellular Carcinoma (20). Consistent with the previously published papers, the high expression of PSMD14 and CCT6A were found positively related to the poor prognostic of HCC patients in our research.

Enrichment analysis revealed many significantly enriched pathways for the signature, of which most were metabolism related. To further investigate the functions of PSMD14 and its associated genes in HCC, we performed GSEA using TCGA data, GSEA showed that purine metabolism, pyrimidine metabolism and ubiquitin mediated proteolysis are differentially enriched between PSMD14 gene high expression and PSMD14 associated genes high risk phenotype. Besides, glycine serine and threonine metabolism, primary bile acid biosynthesis and retinol metabolism are differentially enriched between PSMD14 gene low expression and PSMD14 associated genes low risk phenotype.

Another important aspect of this study, seven genes mRNA expression was correlated with diverse immune infiltration levels in LIHC. PSMD14, RBM45, PSMD1, OLA1 and CCT6A mRNA expression level was significantly positively correlated with infiltrating levels of B Cell, CD8+ T cell, CD4+ T cell, Macrophage, Neutrophils and Dendritic cells. In addition, LCAT mRNA expression had a significantly negative correlation with infiltrating levels of tumor purity, B Cell, CD8+ T cell, CD4+ T cell, Macrophage, Neutrophils and Dendritic cells. IVD mRNA expression was significantly positive related to tumor purity and had a significantly negative correlation with infiltrating levels of B Cell, CD8+ T cell, CD4+ T cell, Macrophage and Dendritic cells and no significant correlations with Neutrophils. Moreover, the correlation between seven immune genes expression and the signature genes of immune cells imply the role of its in regulating tumor immunology. Of note, among the 7 genes, only the PSMD14 and CCT6A, have been reported that correlated with diverse immune cells levels. For instance, POH1 deficiency in macrophages resulting in deubiquitination of pro-IL-1β that restrains inflammatory responses for the maintenance of immune homeostasis (23). CCT6A research shown that CD8(+) T cells provide functional in cytokine secretion and lytic activity upon of their cognate antigens, it was used in personalized adoptive T-cell therapy of melanoma (24). These correlations could be indicative of a potential mechanism for 7

immune-related genes regulate immune cells in HCC. The above suggested that PSMD14 and signature genes could play a significant role in recruitment and regulation of immune infiltrating cells in HCC.

Conclusions

We systematically analyzed the expression and prognosis of PSMD14, and screened the immune prognostic genes significantly related to PSMD14 from the open database to construct and verify the immune-related genes. We found that (PSMD14, RBM45, PSMD1, OLA1, CCT6A, LCAT and IVD) are immune prognostic signatures of HCC. Therefore, this study deepens our understanding of HCC IRGs and provides new potential biomarkers for prognosis and treatment.

Abbreviations

AUC: area under the curve; C-index: concordance index; GO: Gene Ontology; GSEA: Gene Set Enrichment Analysis; HR: hazard ratio; KEGG: Kyoto Encyclopedia of Genes and Genomes; TIC: Tumor-infiltrating immune cell; LASSO: least absolute shrinkage and selection operator; HCC: hepatocellular carcinoma; CHOL: Cholangiocarcinoma; FLC: Fibrolamellar Carcinoma; HCC: Hepatocellular Carcinoma; HL: Hepatic Lobectomy; SSLR: single segment liver resection; OS: overall survival; ROC: Receiver Operating Characteristics; TCGA: The Cancer Genome Atlas; ICGC: International Cancer Genome Consortium.

Declarations

Acknowledgements

Not applicable.

Authors' contributions

CT and MA wrote the paper; XRL and HZ assisted in the preparation of the manuscript and editing. XYC and RW coordinated all the research activities, from the design of the experiment to the final correction of the manuscript. All authors have read and approved the final manuscript.

Funding

The work was supported by grants from the National Natural Science Foundation of China (No. 81772995 and 81472266); the Excellent Youth Foundation of Jiangsu Province, China (BK20140032) and Jiangsu Province's Key Provincial Talents Program (No.ZDRCA2016090).

Competing interests

The authors declare that they have no competing interests.

Availability of data and materials

The TCGA, ICGC and Other databases material is public available.

Ethics approval and consent to participate

No ethical approval nor informed consent was required in this study due to the public-availability of the data used.

Consent for publication

Not applicable.

References

1. Rimassa L, Danesi R, Pressiani T, Merle P. Management of adverse events associated with tyrosine kinase inhibitors: Improving outcomes for patients with hepatocellular carcinoma. Cancer Treat. Rev. 2019 Jul;77.
2. Long J, Chen P, Lin J, Bai Y, Yang X, Bian J, Lin Y, Wang D, Yang X, Zheng Y, Sang X, Zhao H. DNA methylation-driven genes for constructing diagnostic, prognostic, and recurrence models for hepatocellular carcinoma. Theranostics 2019;9(24).
3. Shi Y, Men X, Li X, Yang Z, Wen H. Research progress and clinical prospect of immunocytotherapy for the treatment of hepatocellular carcinoma. Int. Immuno pharmacol. 2020 Mar 03;82.
4. Cai MJ, Cui Y, Fang M, Wang Q, Zhang AJ, Kuai JH, Pang F, Cui XD. Inhibition of PSMD4 blocks the tumorigenesis of hepatocellular carcinoma. Gene 2019 Jun 20;702:66-74.
5. Pan L, Fang J, Chen MY, Zhai ST, Zhang B, Jiang ZY, Juengpanich S, Wang YF, Cai XJ. Promising key genes associated with tumor microenvironments and prognosis of hepatocellular carcinoma. World J. Gastroenterol. 2020 Feb 28;26(8).
6. Lv J, Zhang S, Wu H, Lu J, Lu Y, Wang F, Zhao W, Zhan P, Lu J, Fang Q, Xie C, Yin Z. Deubiquitinase PSMD14 enhances hepatocellular carcinoma growth and metastasis by stabilizing GRB2. Cancer Lett. 2020 Jan 28;469.
7. Seo D, Jung SM, Park JS, Lee J, Ha J, Kim M, Park SH. The deubiquitinating enzyme PSMD14 facilitates tumor growth and chemoresistance through stabilizing the ALK2 receptor in the initiation of BMP6 signaling pathway. EBioMedicine 2019 Nov;49.
8. Wang B, Ma A, Zhang L, Jin WL, Qian Y, Xu G, Qiu B, Yang Z, Liu Y, Xia Q, Liu Y. POH1 deubiquitylates and stabilizes E2F1 to promote tumour formation. Nat Commun 2015 Oct 29;6.
9. Wang B, Xu X, Yang Z, Zhang L, Liu Y, Ma A, Xu G, Tang M, Jing T, Wu L, Liu Y. POH1 contributes to hyperactivation of TGF-β signaling and facilitates hepatocellular carcinoma metastasis through deubiquitinating TGF-β receptors and caveolin-1. EBioMedicine 2019 Mar;41.
10. Butler LR, Densham RM, Jia J, Garvin AJ, Stone HR, Shah V, Weekes D, Festy F, Beesley J, Morris JR. The proteasomal de-ubiquitinating enzyme POH1 promotes the double-strand DNA break response.

EMBO J. 2012 Oct 03;31(19).

11. Byrne A, McLaren RP, Mason P, Chai L, Dufault MR, Huang Y, Liang B, Gans JD, Zhang M, Carter K, Gladysheva TB, Teicher BA, Biemann HP, Booker M, Goldberg MA, Klinger KW, Lillie J, Madden SL, Jiang Y. Knockdown of human deubiquitinase PSMD14 induces cell cycle arrest and senescence. Exp. Cell Res. 2010 Jan 15;316(2).
12. Song Y, Li S, Ray A, Das DS, Qi J, Samur MK, Tai YT, Munshi N, Carrasco RD, Chauhan D, Anderson KC. Blockade of deubiquitylating enzyme Rpn11 triggers apoptosis in multiple myeloma cells and overcomes bortezomib resistance. Oncogene 2017 10 05;36(40).
13. Zhu R, Liu Y, Zhou H, Li L, Li Y, Ding F, Cao X, Liu Z. Deubiquitinating enzyme PSMD14 promotes tumor metastasis through stabilizing SNAIL in human esophageal squamous cell carcinoma. Cancer Lett. 2018 04 01;418.
14. Luo G, Hu N, Xia X, Zhou J, Ye C. RPN11 deubiquitinase promotes proliferation and migration of breast cancer cells. Mol Med Rep 2017 Jul;16(1):331-338.
15. Chen X, Cheung ST, So S, Fan ST, Barry C, Higgins J, Lai KM, Ji J, Dudoit S, Ng IO, Van De Rijn M, Botstein D, Brown PO. Gene expression patterns in human liver cancers. Biol. Cell 2002 Jun;13(6).
16. Roessler S1, Jia HL, Budhu A, Forgues M, Ye QH, Lee JS, Thorgeirsson SS, Sun Z, Tang ZY, Qin LX, Wang XW. A unique metastasis gene signature enables prediction of tumor relapse in early-stage hepatocellular carcinoma patients. Cancer Res. 2010 Dec 15;70(24):10202-12.
17. Wurmbach E, Chen YB, Khitrov G, Zhang W, Roayaie S, Schwartz M, Fiel I, Thung S, Mazzaferro V, Bruix J, Bottinger E, Friedman S, Waxman S, Llovet JM. Genome-wide molecular profiles of HCV-induced dysplasia and hepatocellular carcinoma. Hepatology 2007 Apr;45(4).
18. Tan Y, Jin Y, Wu X, Ren Z. PSMD1 and PSMD2 regulate HepG2 cell proliferation and apoptosis via modulating cellular lipid droplet metabolism. BMC Mol. Biol. 2019 11 08;20(1).
19. Huang S, Zhang C, Sun C, Hou Y, Zhang Y, Tam NL, Wang Z, Yu J, Huang B, Zhuang H, Zhou Z, Ma Z, Sun Z, He X, Zhou Q, Hou B, Wu L. Obg-like ATPase 1 (OLA1) overexpression predicts poor prognosis and promotes tumor progression by regulating P21/CDK2 in hepatocellular carcinoma. Aging (Albany NY) 2020 Feb 11;12(3):3025-3041.
20. Zeng G, Wang J, Huang Y, Lian Y, Chen D, Wei H, Lin C, Huang Y. Overexpressing CCT6A Contributes To Cancer Cell Growth By Affecting The G1-To-S Phase Transition And Predicts A Negative Prognosis In Hepatocellular Carcinoma. Onco Targets Ther 2019;12.
21. Long J, Chen P, Lin J, Bai Y, Yang X, Bian J, Lin Y, Wang D, Yang X, Zheng Y, Sang X, Zhao H. DNA methylation-driven genes for constructing diagnostic, prognostic, and recurrence models for hepatocellular carcinoma. Theranostics 2019;9(24).
22. Spataro V, Toda T, Craig R, Seeger M, Dubiel W, Harris AL, Norbury C. Resistance to diverse drugs and ultraviolet light conferred by overexpression of a novel human 26 S proteasome subunit. Biol. Chem. 1997 Nov 28;272(48).

23. Zhang L, Liu Y, Wang B, Xu G, Yang Z, Tang M, Ma A, Jing T, Xu X, Zhang X, Liu Y. POH1 deubiquitinates pro-interleukin-1β and restricts inflammasome activity. Nat Commun 2018 10 12;9(1).
24. Höfflin S, Prommersberger S, Uslu U, Schuler G, Schmidt CW, Lennerz V, Dörrie J, Schaft N. Generation of CD8(+) T cells expressing two additional T-cell receptors (TETARs) for personalised melanoma therapy. Cancer Biol. Ther. 2015;16(9).

Tables

Table 1. TCGA hepatic carcinoma patient characteristics

Clinical characteristics		Total (418)	%
Age at diagnosis (y)		61(16-90)	
Gender	Male/ Female	272/146	65.1/34.9
Histologic grade	Well/Moderate/Poor	55/304/13	14.8/81.7/3.5
Status	With tumor/Tumor free	133/254	34.4/65.6
TNM Stage	I/II/III/IV	194/98/90/12	49.2/24.9/22.8/3.1
Grade	I/II/III/IV	55/180/124/13	14.8/48.4/33.3/3.5
Vascular invasion	Macro/ Micro/ No	17/94/210	5.3/29.3/65.4
Risk Factors	Hepatitis B/ Other	78/222	26.0/74.0
Histology	Hepatocellular Carcinoma	367	87.8
	Cholangiocarcinoma	41	9.8
	Hepatocholangiocarcinoma (Mixed)	7	1.7
	Fibrolamellar Carcinoma	3	0.7
Tumor size	≤5cm	311	74.9
	>5cm	104	25.1
Lymph nodes	Negative/ Positive	290/8	97.3/2.7
Distant metastasis	Negative/ Positive	303/8	97.4/2.6

Table 2. PSMD14 expression aassociated with clinical pathological characteristics from TCGA (logistic regression)

Clinical characteristics	Total (N)	Odds ratio in PSMD14 expression	p-Value
Age	376	0.99 (0.98-1.01)	0.444
BMI	341	0.99 (0.96-1.01)	0.409
Gender (female vs. male)	377	1.02(0.66-1.57)	0.941
Grade (well vs. moderate)	359	1.91(1.06-3.51)	0.033
Histology (FLC vs. HCC)	370	0.48(0.02-5.06)	0.552
Status (tumor free vs. with tumor)	349	0.90(0.57-1.41)	0.644
Vascular invasion (positive vs. negative)	321	0.73(0.45-1.16)	0.180
Hepatitis B(positive vs. negative)	300	0.84(0.49-1.41)	0.504
Stage (I vs. II or III)	353	2.51 (1.25-4.32)	0.001
Surgical approach(HL vs. SSLR)	113	0.26 (0.09-0.67)	0.007
Tumor size(≤5cm vs. >5cm)	374	1.65 (1.03-2.67)	0.039
Distant metastasis (positive vs. negative)	276	1.00 (0.12-8.43)	1.000
Lymph nodes (positive vs. negative)	261	3.05 (0.38-62.07)	0.337

FLC: Fibrolamellar Carcinoma; HCC: Hepatocellular Carcinoma; HL: Hepatic Lobectomy;

SSLR: single segment liver resection

Table 3. Univariate and multivariate analyses of overall survival in hepatocellular carcinoma patients of TCGA

Variables	Univariate analysis		Multivariate analysis	
	HR (95% CI)	P-value	HR (95% CI)	P-value
PSMD14	2.17(1.32-3.57)	0.002	1.90(1.08-3.33)	0.026
Age	1.02(0.99-1.05)	0.107	1.02(0.99-1.04)	0.190
Gender	0.60(0.34-1.06)	0.078	0.97(0.51-1.87)	0.936
Vascular invasion	1.27(0.70-2.28)	0.435	0.84(0.44-1.62)	0.606
Grade	1.18(0.80-1.75)	0.400	1.10(0.70-1.74)	0.677
Status	2.65(1.49-4.72)	0.001	1.91(1.02-3.55)	0.042
Stage	1.72(1.28-2.32)	0.000	0.78(0.15-3.96)	0.764
T stage	1.65(1.24-2.20)	0.001	1.91(0.42-8.67)	0.399
Distant metastasis	4.15(0.99-17.24)	0.050	0.95(0.17-5.18)	0.954
Lymph nodes	3.42(0.47-24.96)	0.226	3.33(0.08-143.94)	0.531

Table 4. The HR and p values of 6 Genes

Gene	Gene description	HR	HR.95L	HR.95H	P value
RBM45	RNA Binding Motif Protein 45	5.022	2.679	9.411	4.74E-07
PSMD1	26S Proteasome Regulatory Subunit S1	2.982	1.978	4.496	1.83E-07
OLA1	Obg Like ATPase 1	2.213	1.603	3.055	1.39E-06
CCT6A	Chaperonin Containing TCP1 Subunit6A	2.118	1.564	2.869	1.24E-06
IVD	Isovaleryl-CoA Dehydrogenase	0.636	0.495	0.816	0.000
LCAT	Lecithin-Cholesterol Acyltransferase	0.775	0.684	0.877	5.63E-05

Note: HR and P values were generated from univariate Cox regression in TCGA dataset

Table 5. Primer sequences used in this study

Primer name	Primer sequences (5'→3')
GAPDH-OF	GAACGGGAAGCTCACTGG
GAPDH-OR	GCCTGCTTCACCACCTTCT
IVD-OF	ATGGCAGAGATGGCGACTG
IVD-OR	TAGCCCATTGATTGCATCGTC
LCAT-OF	ACCTGGTCAACAATGGCTACG
LCAT-OR	TAGAGCAAGTGTAGACAGCCG
CCT6A-OF	TGACGACCTAAGTCCTGACTG
CCT6A-OR	ACAGAACGAGGGTTGTTACATTT
OLA1-OF	TTGCAGCACTCCAACTAGAATAC
OLA1-OR	TCGGTTGTTGAGGTGTGTTAAAT
PSMD1-OF	TCCGAGTCCGTAGACAAAATAGA
PSMD1-OR	CCACACATTGTTTGGTGTAGTGA
PSMD14-OF	AAGTTATGGGTTTGATGCTTGGA
PSMD14-OR	ATACCAACCAACAACCATCTCC
RBM45-OF	TCAGCAAGTACACACCTGAGT
RBM45-OR	AGATGATCGGGACTGAGCAAT

Figures

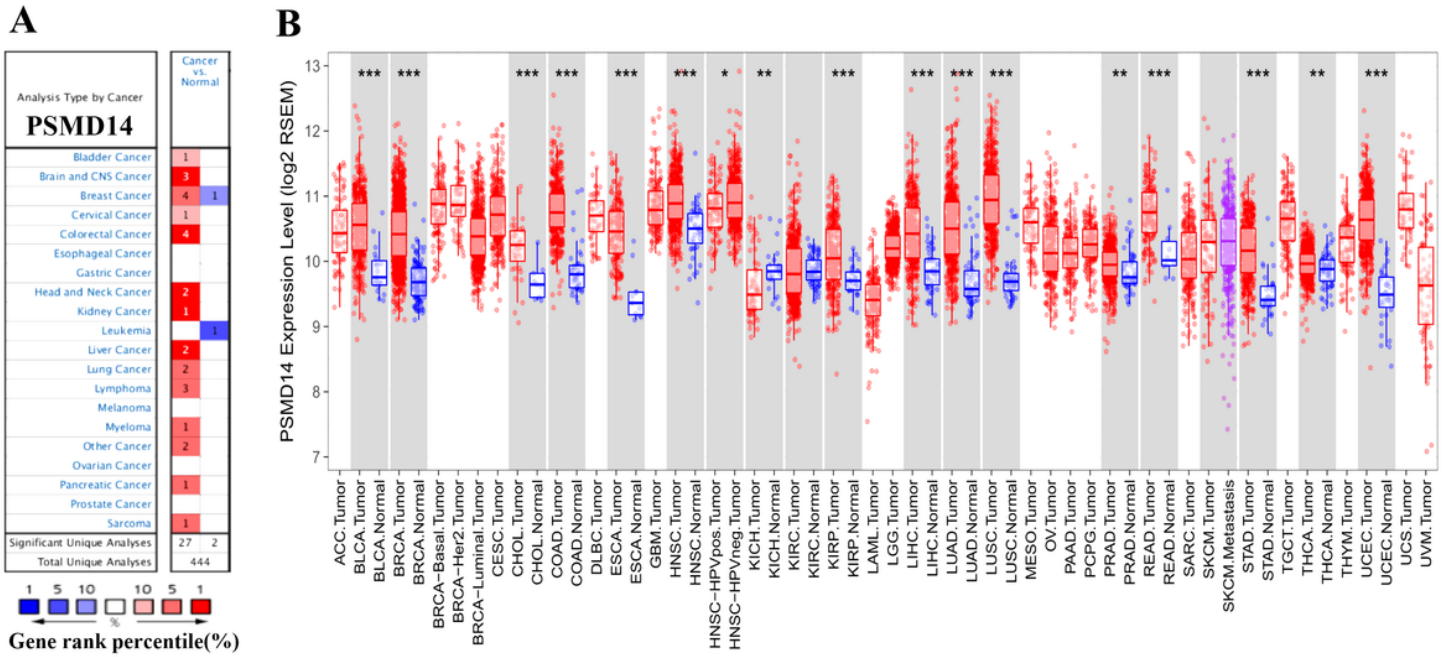

Figure 1

PSMD14 expression levels in human cancers. (A) PSMD14 in data sets of different cancers in the Oncomine database. (B) PSMD14 expression levels in different tumor types were determined by TIMER (*P < 0.05, **P <0.01, ***P < 0.001).

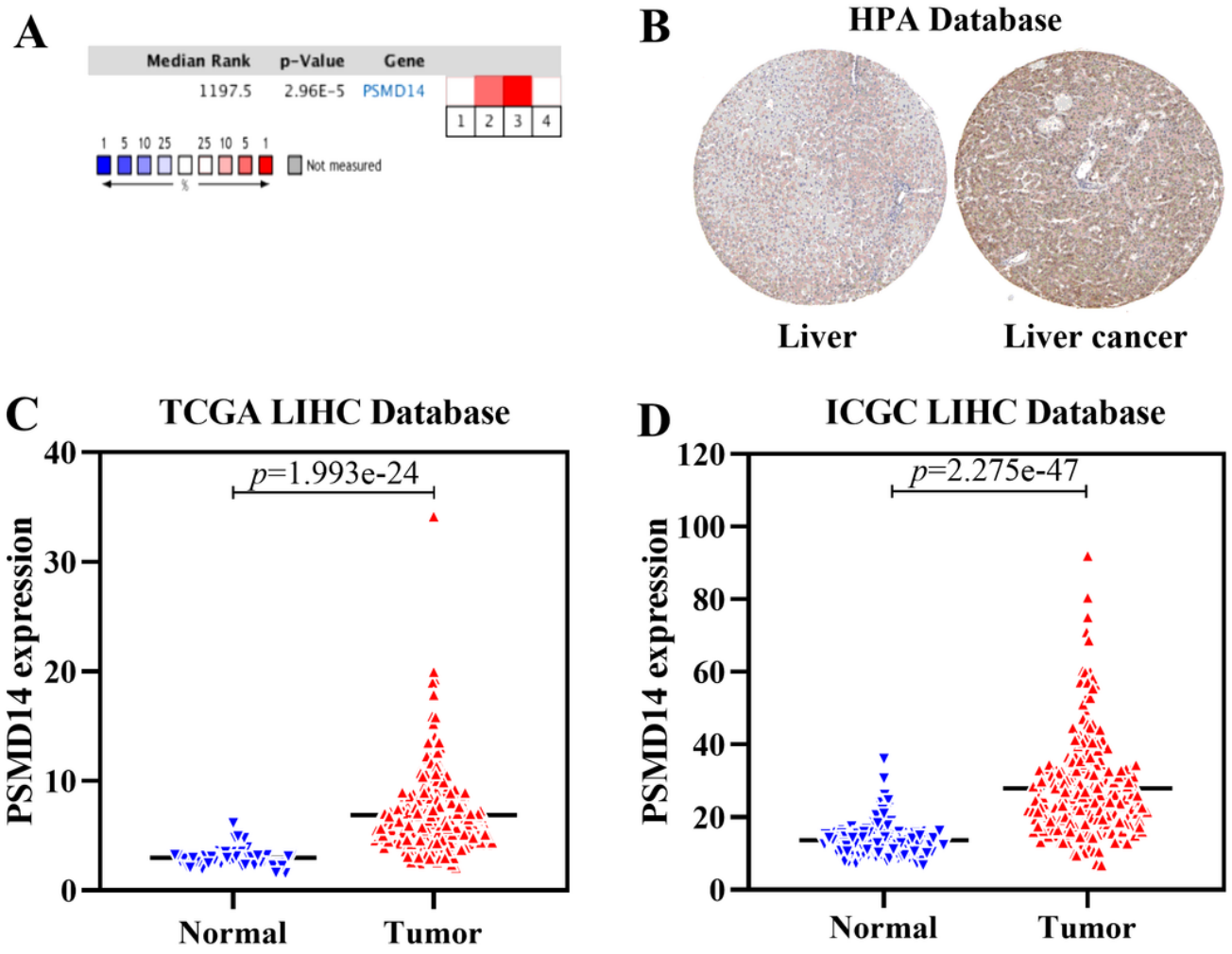

Figure 2

PSMD14 expression is upregulated in HCC. (A) A meta-analysis of PSMD14 gene expression from four Oncomine databases where colored squares indicate the median rank for PSMD14 (vs. Normal tissue) across 4 analyses. Chen Liver (1), Roessler Liver (2-3), Wurmbach Liver (4). The P value is given for the medianrank analysis. (B) The representative protein expression of the PSMD14 in HCC and normal liver tissue. Data were from the Human Protein Atlas (http://www.proteinatlas.org) database. (C) PSMD14 significantly increased in human 374 LIHC tissues to 50 normal tissues using TCGA Database. (D) PSMD14 significantly increased in human 243 LIHC tissues to 202 normal tissues using ICGC Database (*P < 0.05, **P <0.01, ***P < 0.001).

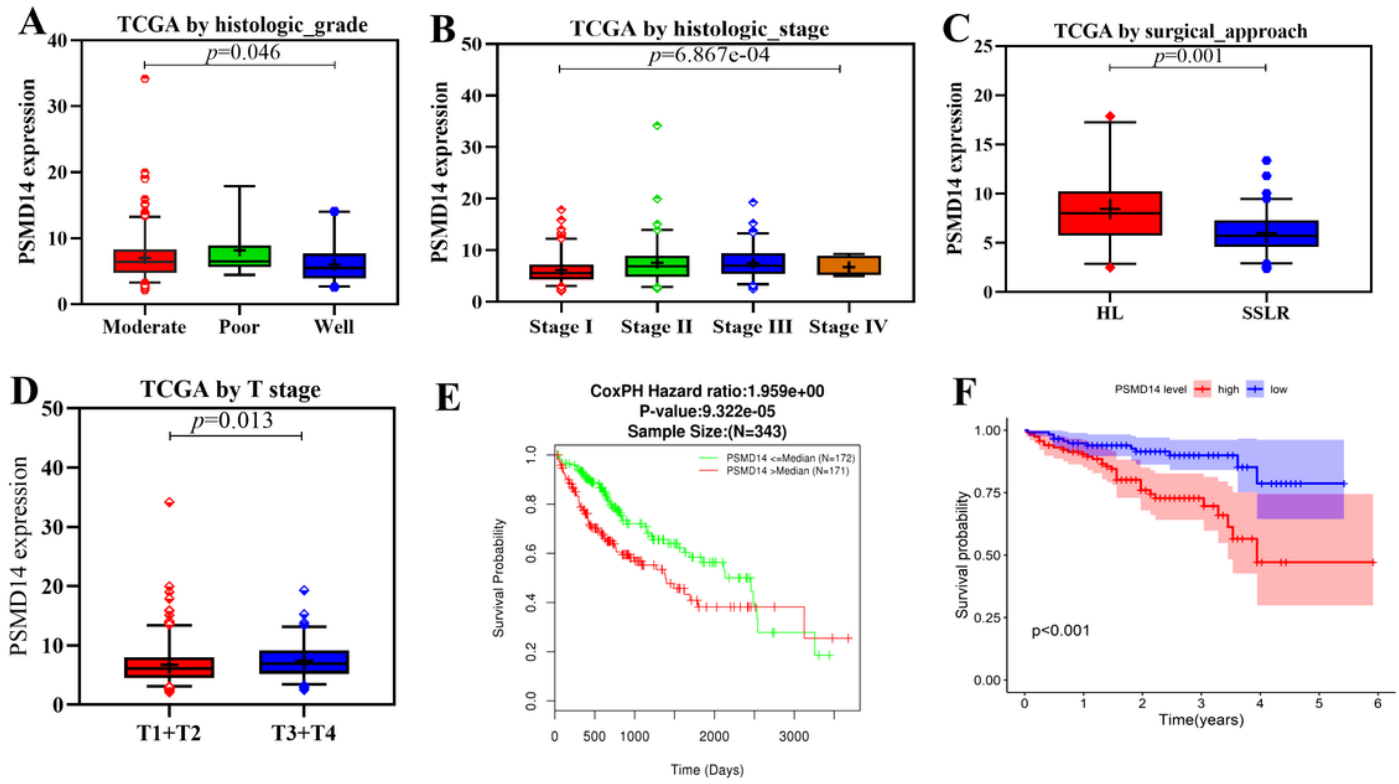

Figure 3

Association with PSMD14 expression and clinicopathologic characteri- stics. including A: histologic grade, B: histologic stage, C: surgical approach, D: T stage. E-F: Impact of PSMD14 expression on overall survival in HCC patients in LinkedOmics and ICGC cohort. ICGC: International Cancer Genome Consortium; HL: Hepatic Lobectomy; SSLR: single segment liver resection.

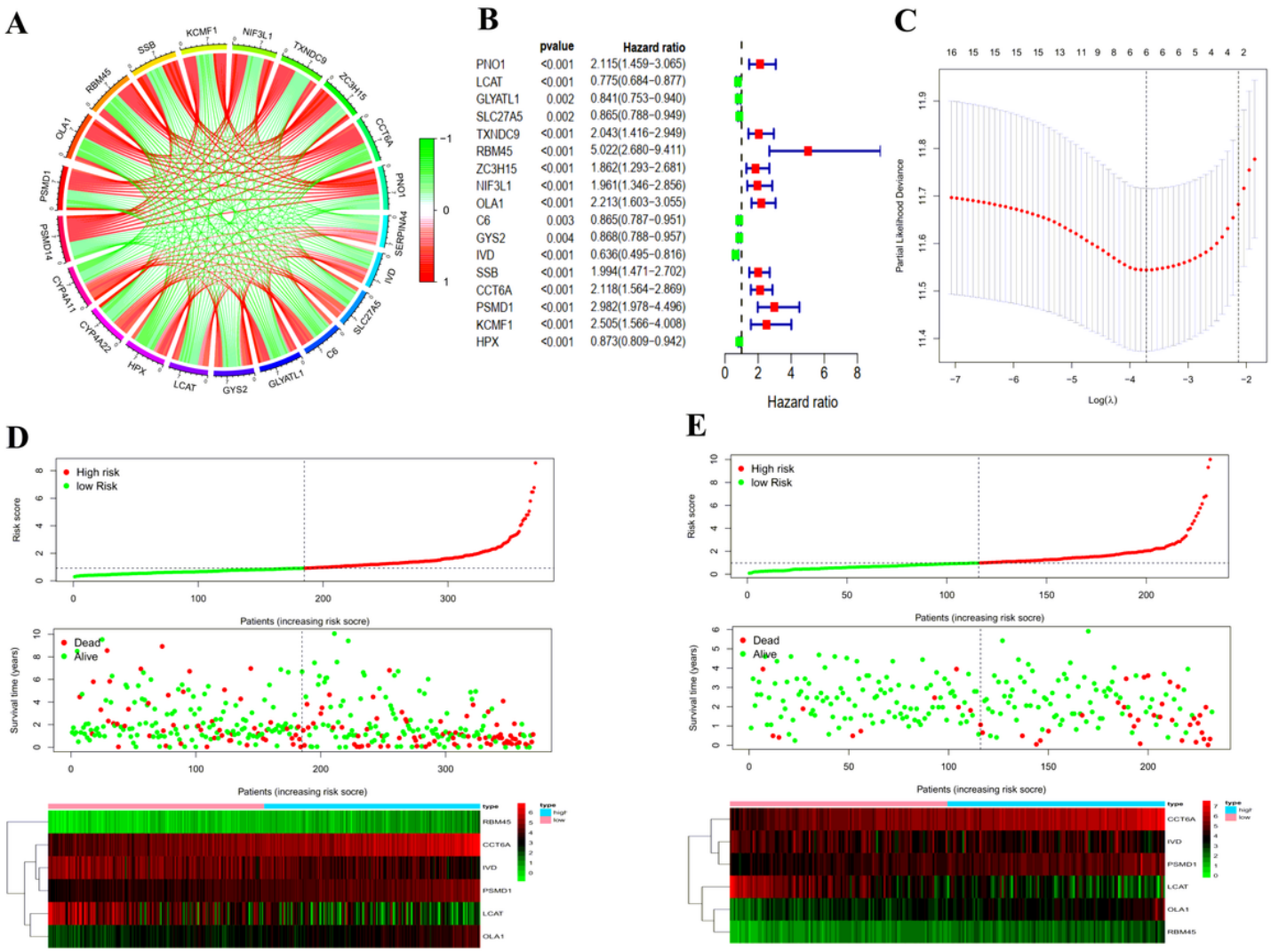

Figure 4

Establishment and validation of the six genes prognostic signature. (A) Circle chart showing PSMD14 related genes (top 10 positive and negative related genes). (B-C) The procedure of the establishment of the prognostic signature. (D) Correlation between the prognostic signature and the overall survival of patients in the TCGA cohort (D) and ICGC (E) cohorts. The distribution of risk scores (upper), survival time (middle) and genes expression levels (below). The black dotted lines represent the median risk score cut-off dividing patients into low- and high-risk groups. The red dots and lines represent the patients in high-risk groups. The green dots and lines represent the patients in low-risk groups.

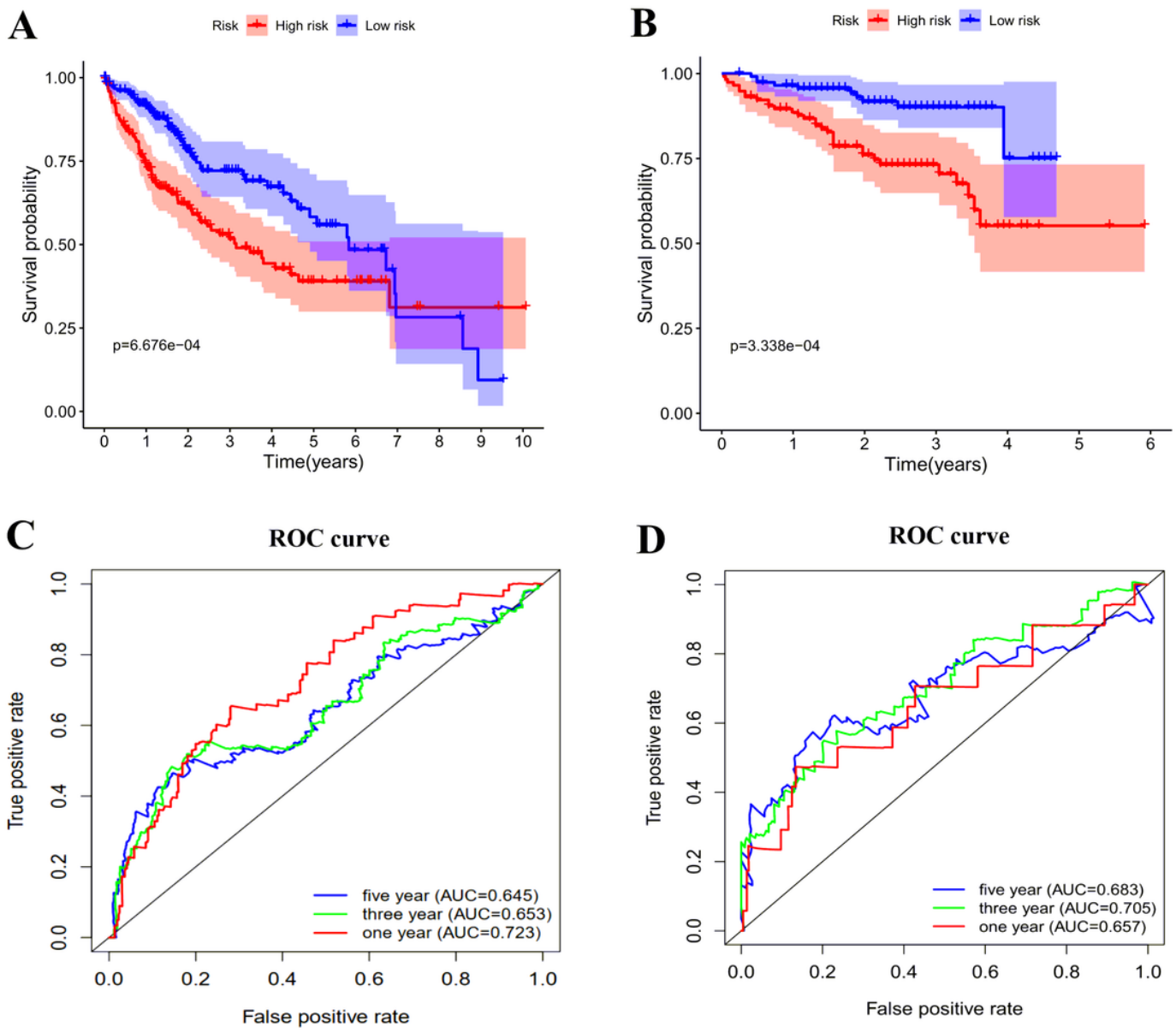

Figure 5

Kaplan-Meier survival and ROC curves of the six genes prognostic signature. (A,B) Kaplan-Meier survival curves of overall survival among risk stratification groups in the TCGA (A) and ICGC (B) set. (C,D) ROC curves with calculated AUCs for risk prediction in 1-, 3-, 5-years in the TCGA (C) and ICGC(D) sets.

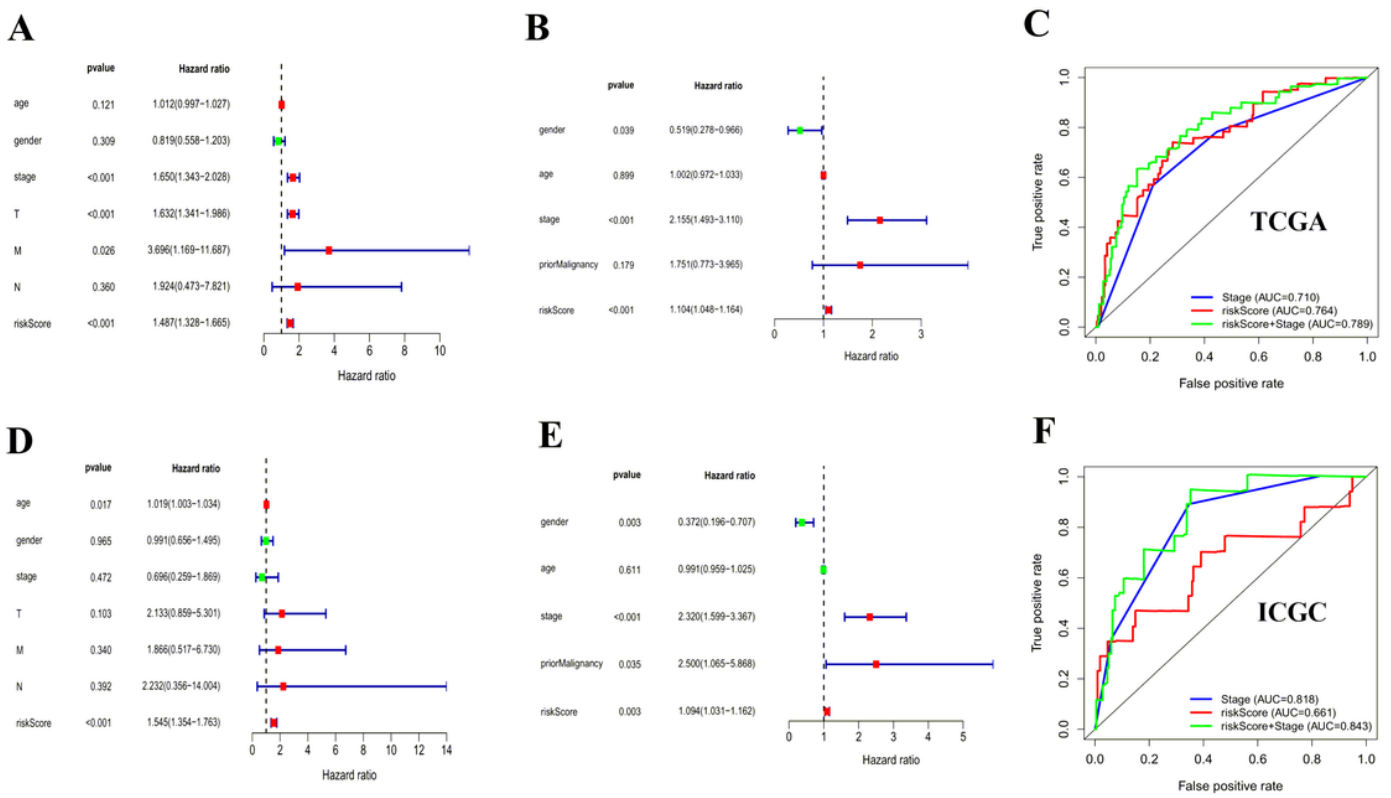

Figure 6

Univariate and multivariate Cox regression analyses of clinical factors associated with overall survival. (A-D) Univariate Cox regression analyses of clinical factors associated with overall survival in the TCGA (A) and ICGC (D) set. (B-E) Multivariate Cox regression analyses of clinical factors associated with overall survival in the TCGA (B) and ICGC (E) sets. The combination of stage and risk score could better predict prognosis in TCGA-LIHC (C) and ICGC-LIHC (F) than either one alone.

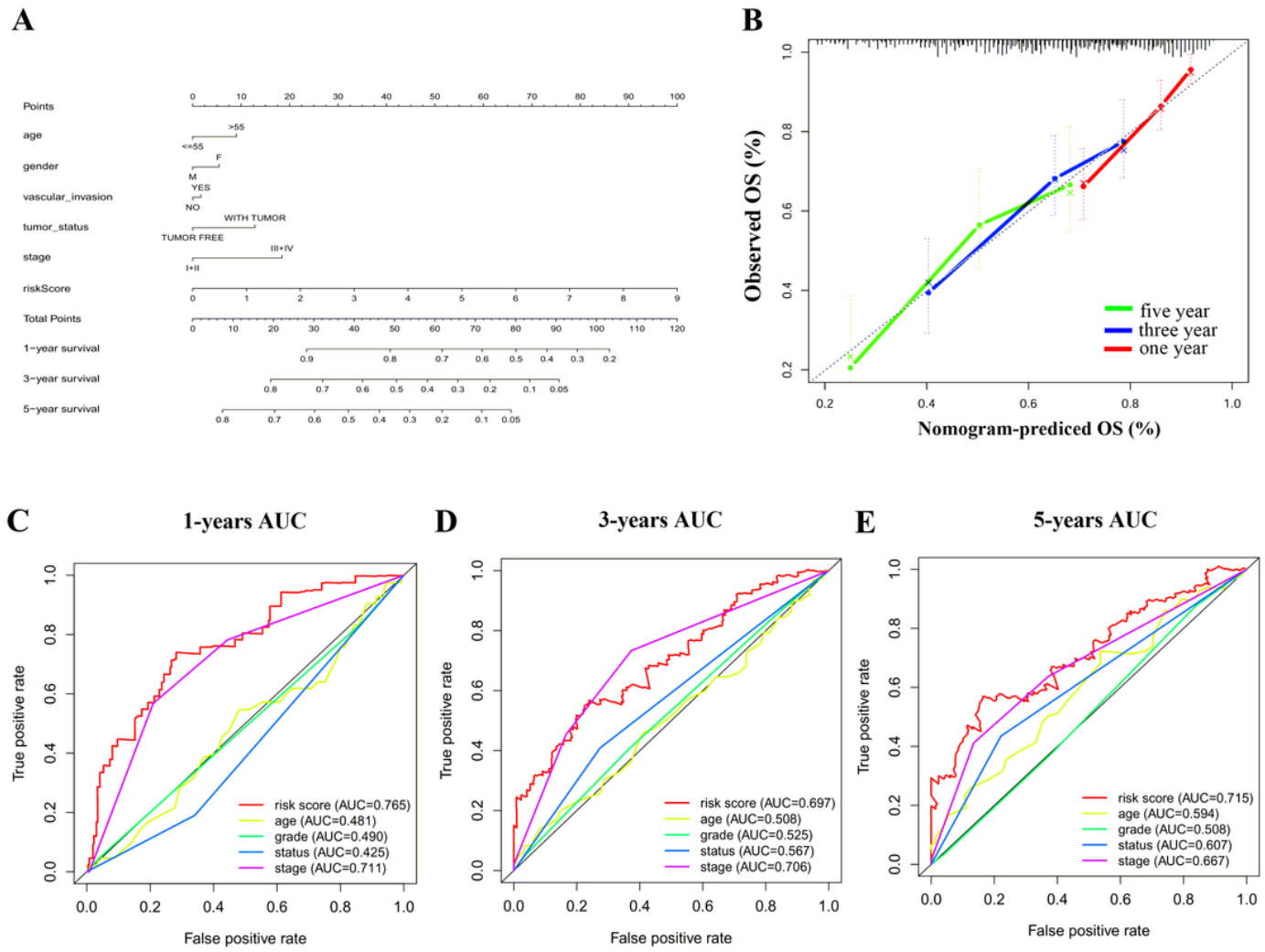

Figure 7

Construction of a nomogram for overall survival prediction in HCC. (A) The nomogram consists of age,gender, grade, vascular invasion,tumor status,stage and the risk score based on the six genes signature. (B) Calibration curves of the nomogram for the estimation of survival rates at 1-, 3-, 5year. (C-E) The Kaplan-Meier curves of the risk subgroups stratified by the tertiles of total points derived from the nomogram.

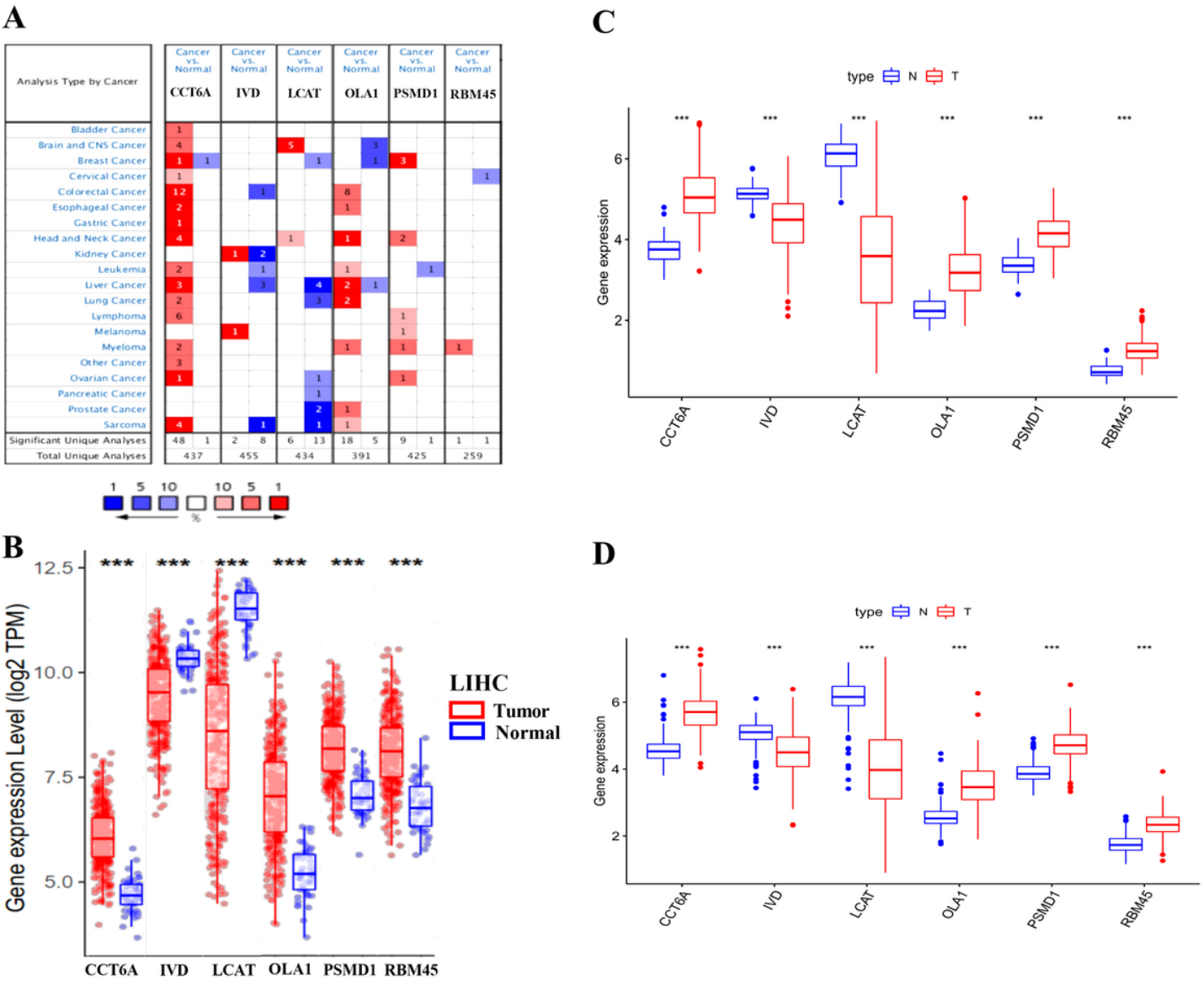

Figure 8

Expression of the six predictive genes in HCC. (A) The expression profiles of the six genes in the Oncomine database. Data of PSMD1 and RBM45 in liver cancer were not found in the database. (B)The expression of the six predictive genes in TIMER-LIHC database. (C-D) The expression of six predictive genes in TCGA-LIHC and ICGC-LIHC database.

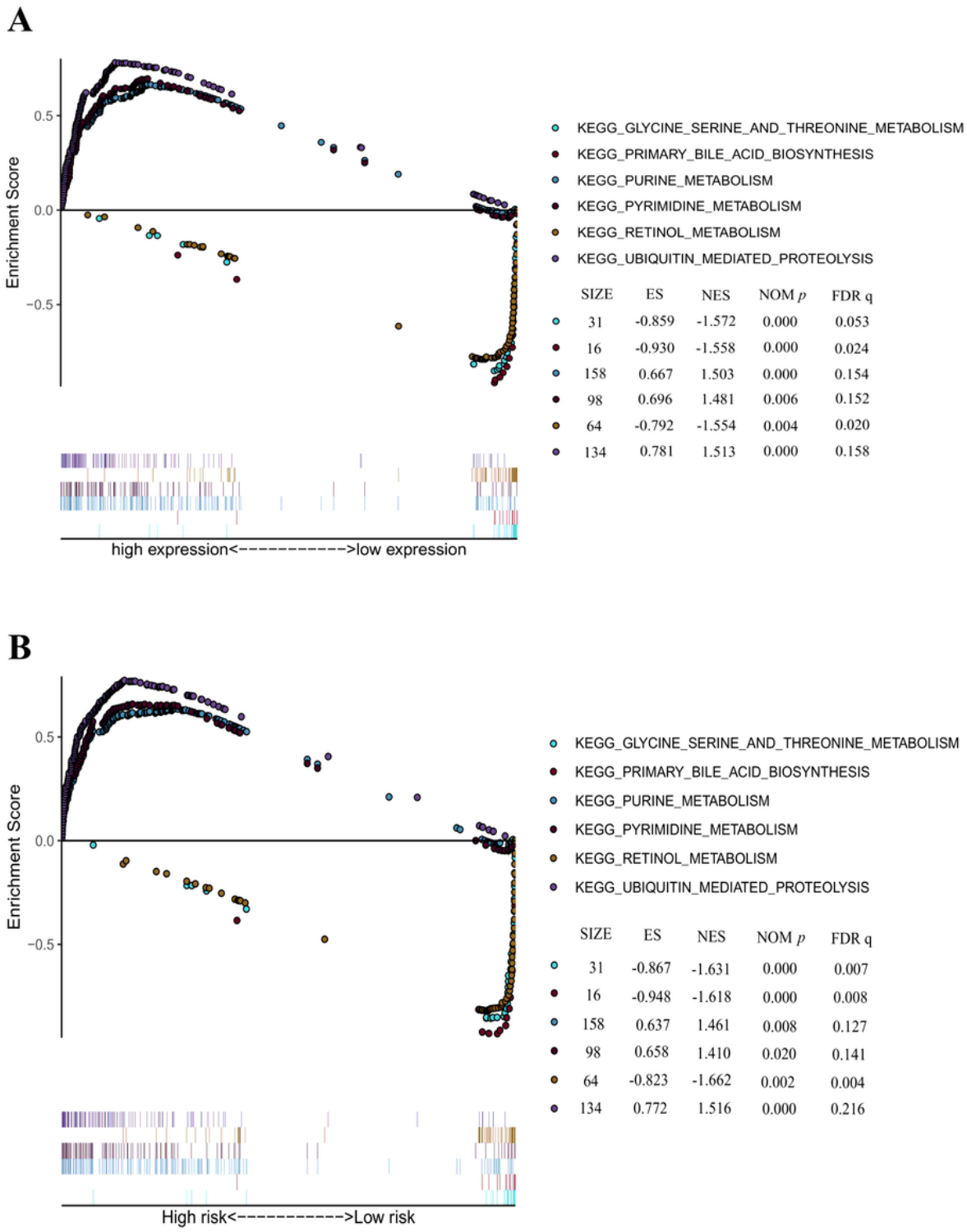

Figure 9

The significantly enriched KEGG pathways in TCGA-LIHC database by GSEA. (A) Six representative KEGG pathways in PSMD14 expression. (B) Six representative KEGG pathways in risk model.

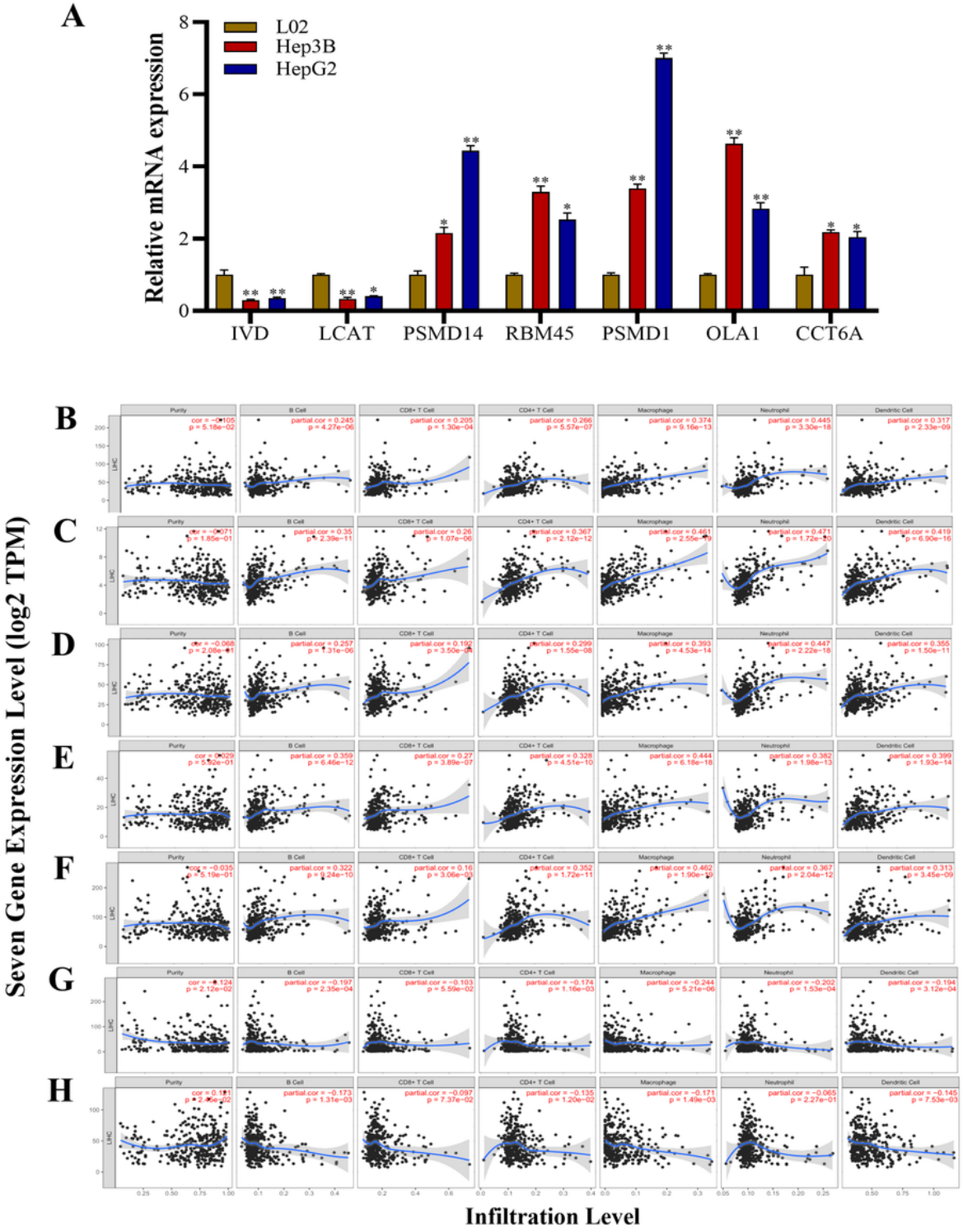

Figure 10

Correlation of seven genes expression with immune infiltration level in LIHC. (A) The levels of seven genes expression were examined in human HCC cell lines Hep3B, HepG2 and the normal liver cell L02. (B-F) PSMD14, RBM45, PSMD1, OLA1 and CCT6A mRNA expression level was significantly positively correlated with infiltrating levels of B Cell, CD8+ T cell, CD4+ T cell, Macrophage, Neutrophils and Dendritic cells. (G) LCAT expression was significantly negatively related to tumor purity and had a

significantly negative correlation with infiltrating levels of B Cell, CD8+ T cell, CD4+ T cell, Macrophage, Neutrophils and Dendritic cells. (H) IVD expression was significantly positive related to tumor purity and had a significantly negative correlation with infiltrating levels of B Cell, CD8+ T cell, CD4+ T cell, Macrophage and Dendritic cells and no significant correlations with Neutrophils.

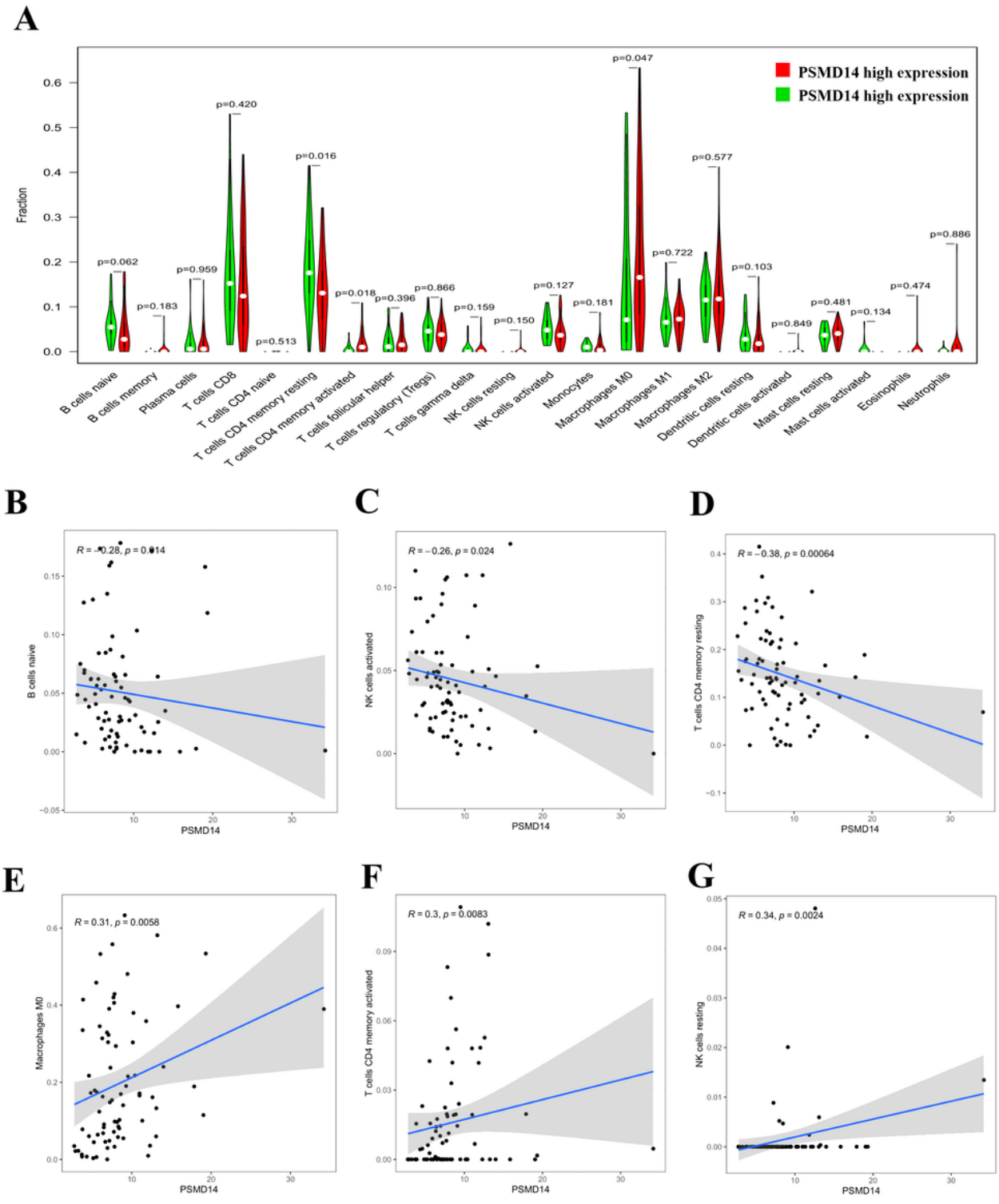

Figure 11

Correlation of TICs proportion with PSMD14 expression. (A) Violin plot showed the ratio differentiation of 21 kinds of immune cells between LIHC tumor samples with low or high PSMD14 expression relative to the median of PSMD14 expression level, and Wilcoxon rank sum was used for the significance test. (B-G) Scatter plot showed the correlation of 6 kinds of TICs proportion with the PSMD14 expression ($p < 0.05$). The blue line in each plot was fitted linear model indicating the proportiontropism of the immune cell along with PSMD14 expression, and Pearson coefficient was used for the correlation test.